Supplementary Information

For the paper 'Subunit organization of the membrane-bound HIV-1 envelope glycoprotein trimer'

Youdong Mao[1], Liping Wang[1], Christopher Gu[1], Alon Herschhorn[1], Shi-Hua Xiang[1,5], Hillel Haim[1], Xinzhen Yang[2], Joseph Sodroski[1,3,4]

[1]Department of Cancer Immunology and AIDS, Dana-Farber Cancer Institute, Department of Microbiology and Immunobiology, Harvard Medical School, Boston, Massachusetts, USA. [2]Division of Viral Pathogenesis, Beth Israel Deaconess Medical Center, Department of Medicine, Harvard Medical School, Boston, Massachusetts, USA. [3]Ragon Institute of MGH, MIT and Harvard, Boston, Massachusetts, USA. [4]Department of Immunology and Infectious Diseases, Harvard School of Public Health, Boston, Massachusetts, USA. [5]Present address: Nebraska Center for Virology, School of Veterinary Medicine and Biomedical Sciences, University of Nebraska-Lincoln, Lincoln, Nebraska, USA. Correspondence should be addressed to

Y.M. (youdong_mao@dfci.harvard.edu) or J.S. (joseph_sodroski@dfci.harvard.edu).

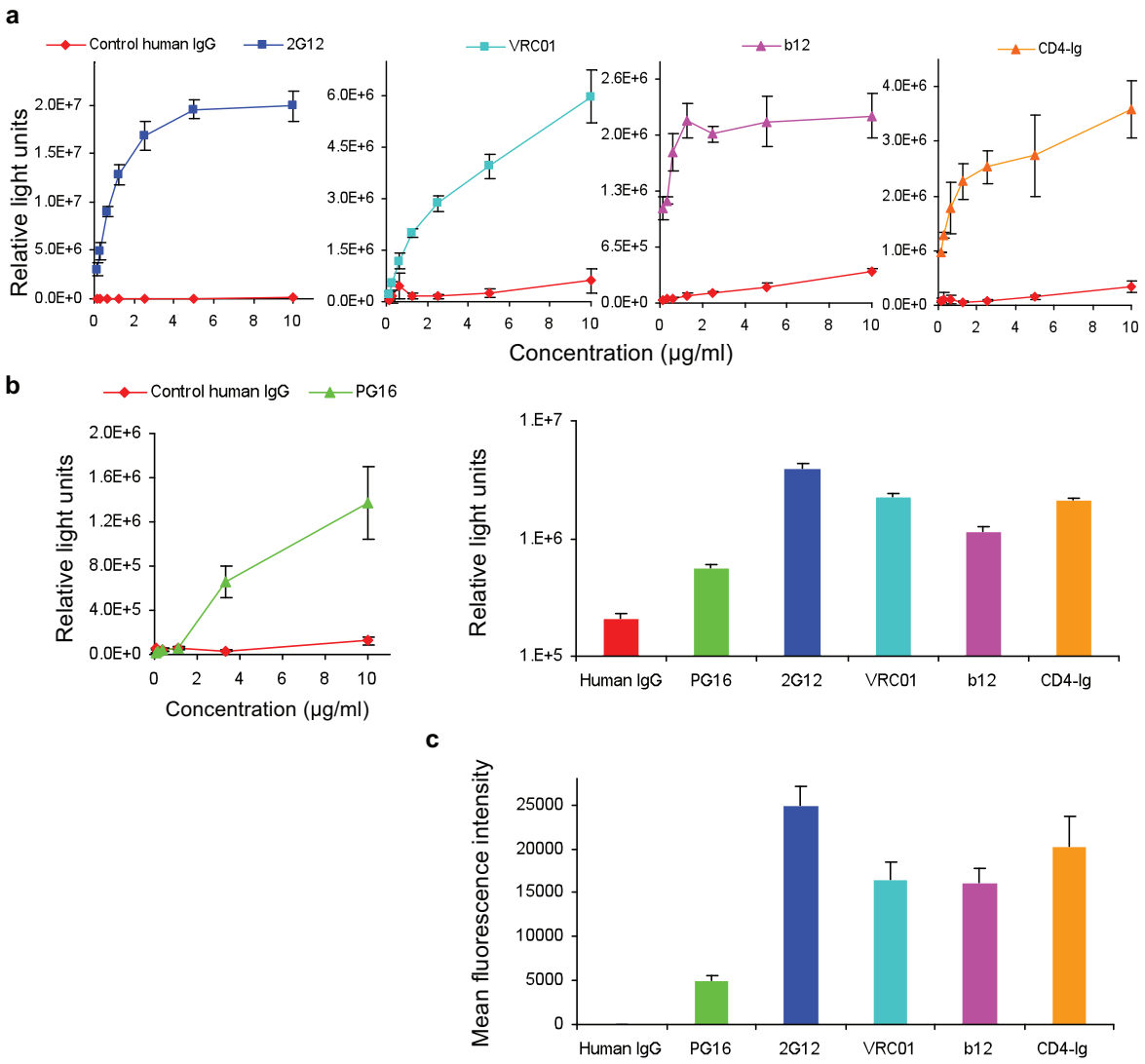

Supplementary Figure 1. Binding of conformation-dependent antibodies and CD4-Ig protein to the purified HIV-1 envelope trimer. **(a)** The binding of different concentrations of 2G12, VRC01, and b12 monoclonal antibodies as well as the CD4-Ig fusion protein to the purified HIV-1_{JR-FL} Env(-)ΔCT trimer was measured by ELISA. Polyclonal human IgG served as a negative control. **(b)** The binding of ligands to the purified HIV-1_{JR-FL} Env(-)ΔCT E168K trimer was measured by ELISA. On the left, a dose-response curve for the binding of the quaternary structure-dependent antibody, PG16, to the Env(-)ΔCT E168K trimer is shown. On the right, the binding of a panel of ligands at a single concentration of 10 μg/ml to the purified Env(-)ΔCT E168K trimer is shown. **(c)** The binding of the indicated Env ligands at a single concentration of 10 μg/ml to the HIV-1_{JR-FL} Env(-)ΔCT E168K trimer expressed on the surface of 293T cells was measured by flow cytometry. The mean fluorescence intensity associated with the binding of the polyclonal human IgG negative control was 32 ± 2.6, too low to be seen on the bar graph. The results shown are representative of those obtained in three to four independent experiments. Note that the general pattern of ligand binding to the purified Env(-)ΔCT E168K trimer **(b)** is similar to that seen for binding to the trimer on the surface of expressing cells **(c)**.

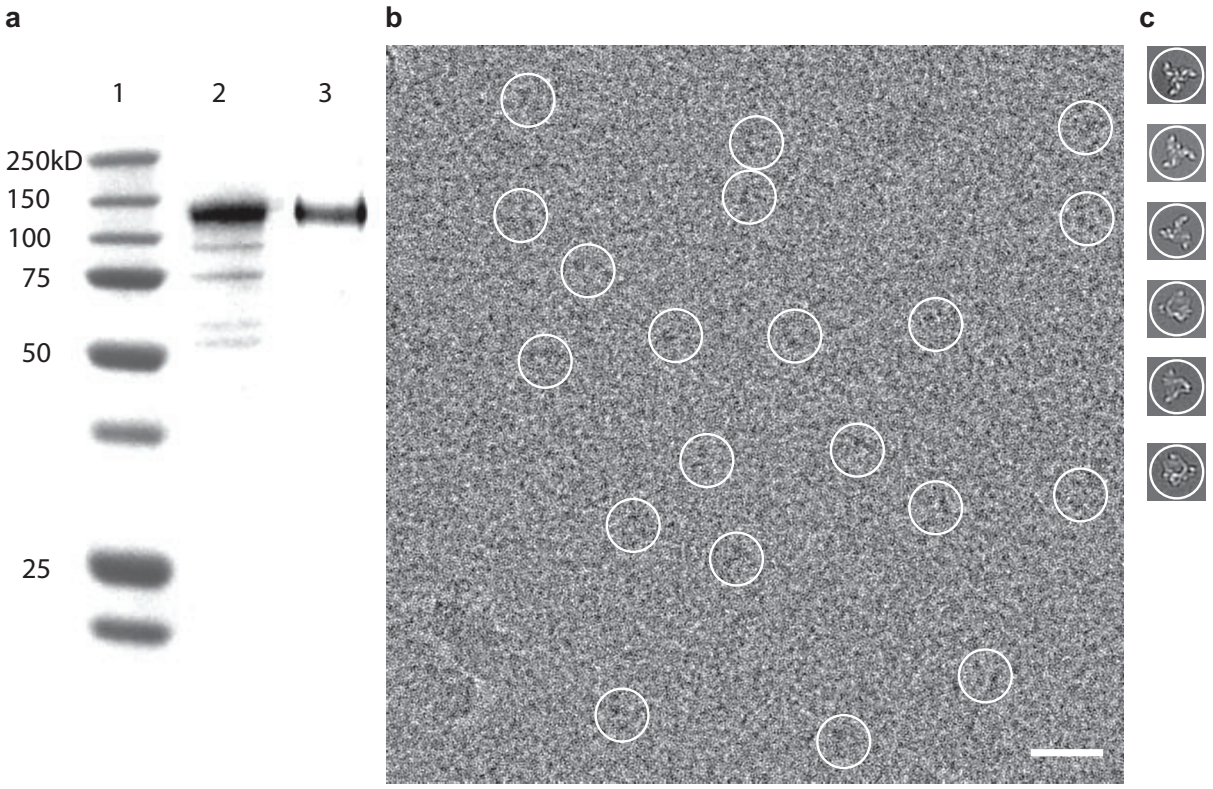

Supplementary Figure 2. Cryo-EM imaging and averaging. (**a**) The Coomassie Blue-stained SDS-polyacrylamide gel shows the Env(-)ΔCT glycoprotein purified from enriched plasma membranes (lane **3**) and from detergent-solubilized cells without separating plasma membranes (lane **2**). Lane **1** shows the markers. The results suggest that the separation of plasma membranes prior to the purification of the Env(-)ΔCT glycoprotein is a necessary step for obtaining a high-quality preparation. (**b**) The image shows a typical 4k-by-4k micrograph of the purified HIV-1_{JR-FL} Env(-)ΔCT trimers protected by the Cymal-6 detergent and embedded in a vitreous ice film. The micrograph shown is low-pass filtered at 1.0 nm. A number of candidate single-particle projections of the Env trimer are highlighted by white circles. Defocus of the micrograph is ~2 μm. Scale bar, 30 nm. (**c**) A number of typical class averages of the molecular projections are shown in the same length scale as **b**, obtained by maximum-likelihood refinement of raw single-particle images without any symmetry imposed (see **Supplementary Fig. 3** for more details). Note that in the micrograph **(b)**, the real particles appear as dark matter because they scatter electrons more strongly than the surrounding amorphous ice or detergent micelles. In **c**, the contrast of single particles is inverted prior to image processing, where protein density appears as bright areas, in accordance with the convention of single-particle reconstruction techniques[19-21]. Because of the requirement to use a specific detergent to preserve the conformational integrity of the membrane-bound Env trimer, the image contrast of single-particle projections in the raw micrograph is rather low, as shown in **b.** The detergents surrounding the Env trimer contribute to the background noise, in addition to the noise from pure vitreous ice. With image alignment and class averaging, the image contrast of single particles can be recovered to a sufficient degree, as shown in **c**, to allow successful 3D reconstruction.

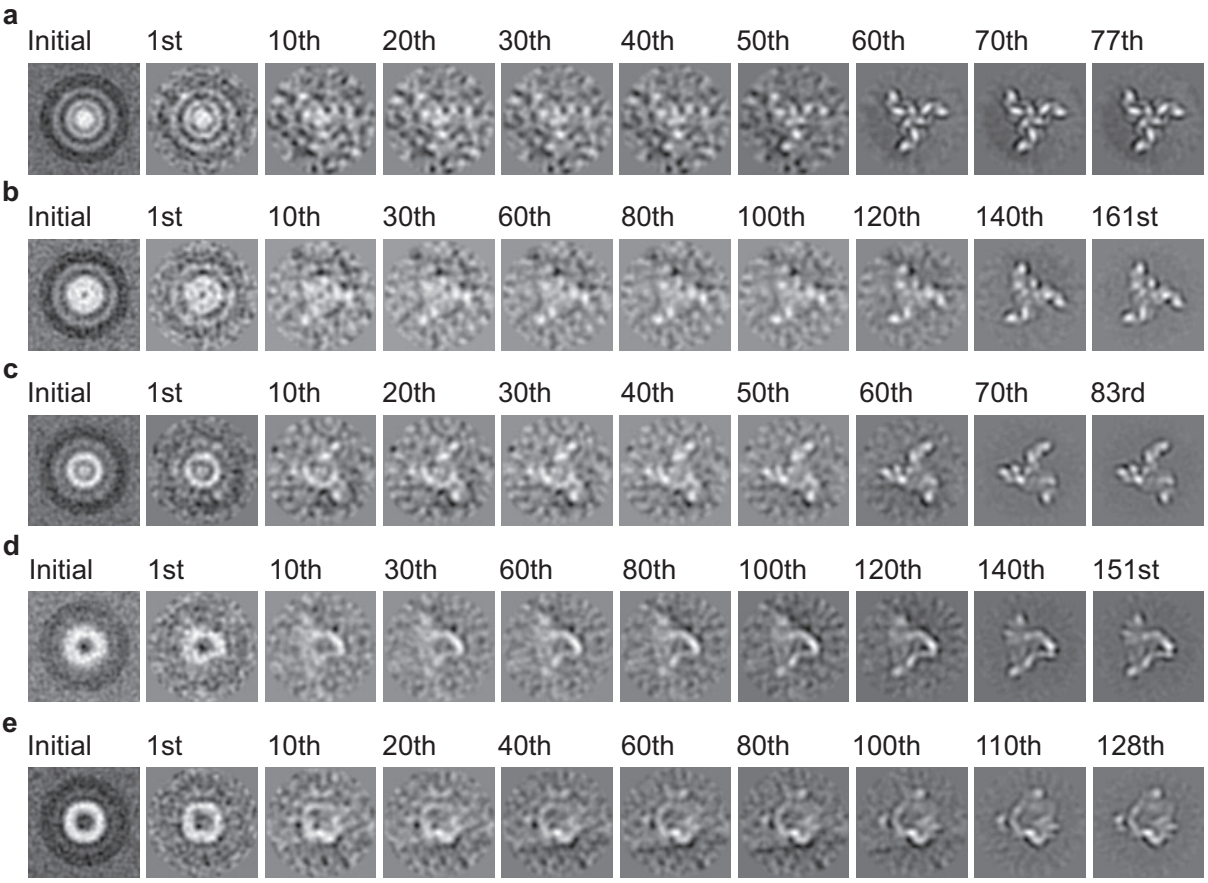

Supplementary Figure 3. Reference-free maximum-likelihood (ML) 2D refinement of class averages. (**a**-**e**) Five typical cases are shown of reference-free ML 2D refinement of projection averages, each of which displays a different view of the Env trimer. Each row shows a sequence of average images from the same projection class, progressing from the initial average to the converged average. The ML 2D refinements started without any external or prior reference images and did not assume any symmetry. The first (leftmost) image is an average of a randomly selected subset of the raw single-particle images in the same class without any alignment against in-plane rotation and x/y shift. This un-aligned average was then used as an initial template for subsequent iterative ML optimization calculations to search for the best alignment parameters (in-plane rotational angle and x/y shift) of the single-particle images. The last (rightmost) image is the class average of the converged iteration where the alignment parameters show no further improvement over those in the previous refinement cycle. Therefore, the last class average in each row demonstrates the greatest contrast of the projection structure. The images in between show the gradual improvement of both the image contrast and the clarity of structural features, with the corresponding number of iterations indicated above each image. Two complete sequences of 2D refinement, corresponding to **a** and **d**, are assembled into **Supplementary Movies 2** and **3**. These ML-refined 2D class averages were used to perform angular reconstitution of the 3D structure. The numbers of single-particle images in the projection classes of **a**, **b**, **c**, **d** and **e** are 4420, 3164, 3556, 2171 and 2529, respectively.

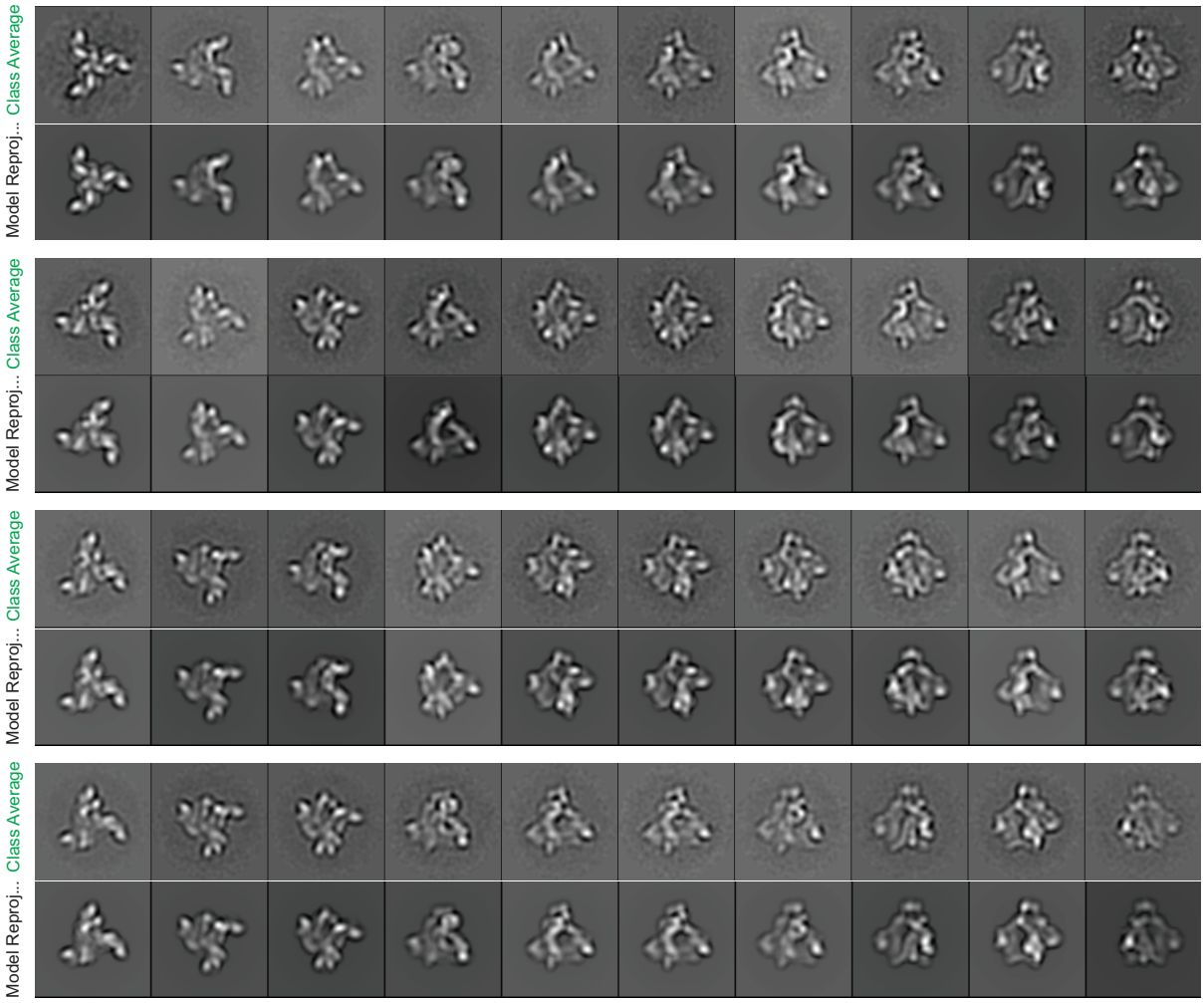

Supplementary Figure 4. Comparison of the class averages refined by a maximum-likelihood (ML) approach and the re-projection of the reconstructed 3D model. The ML-aligned 2D class averages are shown in the 1st, 3rd, 5th, and 7th rows. The corresponding model re-projections are shown in the 2nd, 4th, 6th and 8th rows. The good agreement of the class averages and the model re-projections supports the validity of the 3D reconstruction.

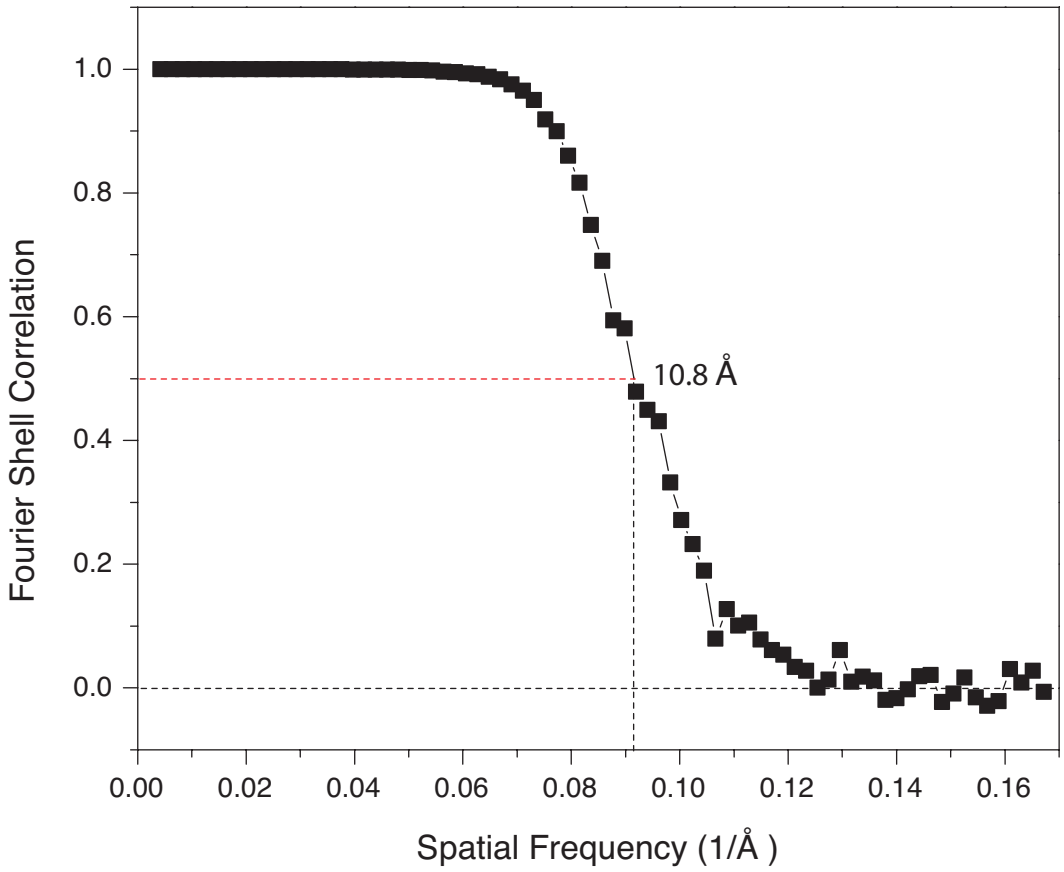

Supplementary Figure 5. Resolution measurement of the cryo-EM structure of the Env(-)ΔCT trimer, using the Fourier shell correlation (FSC) approach and the FSC-0.5 criterion[22]. The FSC was calculated between two separate reconstructions, each generated from a randomly divided half of the entire dataset. The resolution measurement is consistent with the more detailed features that are observed in the structure, compared with previously published lower-resolution maps of the Env trimer[13-15,17,18].